Direct Trace Fitting of Experimental Data Using the Master Equation: Testing Theory and Experiments on the OH + C_2H_4 Reaction

D.J. Medeiros[1], S.H. Robertson[2*], M.A. Blitz[1,3], P.W. Seakins[1*]

1) School of Chemistry, University of Leeds, Leeds, LS2 9JT, UK

2) Dassault Systèmes, 334 Science Park, Milton Rd, Cambridge, CB4 0WN, UK

3) NCAS, University of Leeds, Leeds, LS2 9JT, UK

* To whom correspondence should be addressed; struanhrobertson@gmail.com, p.w.seakins@leeds.ac.uk.

Abstract

Laser flash photolysis coupled with laser induced fluorescence observation of OH has been used to observe the equilibration of OH + C_2H_4 ↔ HOC_2H_4 over the temperature range 563 – 723 K and pressures of bath gas (N_2) from 58 – 250 Torr. The time-resolved OH traces have been directly and globally fitted with a master equation in order to extract $\Delta_R H_0^0$, the binding energy of the HOC_2H_4 adduct, with respect to reagents. The global approach allows the role that OH abstraction plays at higher temperatures to be identified. The resultant value of$\Delta_R H_0^0$,111.8 kJ mol^{-1}, is determined to better than 2 kJ mol^{-1}, and is in agreement with our *ab initio* calculations (carried out at the CCSD(T)/CBS//M06-2X/aug-cc-pVTZ level), of 111.4 kJ mol^{-1}, and other state of the art calculations. Parameters for the abstraction channel are also in good agreement with previous experimental studies. To effect this analysis, the MESMER master equation code was extended to directly incorporate secondary chemistry: diffusional loss from the observation region and reaction with the photolytic precursor. These extensions, which, among other things, resolve issues related to the merging of chemically significant and internal energy relaxation eigenvalues, are presented.

Introduction

The rate coefficients of forward and reverse reactions can be used to determine important thermodynamic parameters.[1] In general, this is achieved by processing the raw experimental data (e.g. concentration of reactants/products as a function of time, often under pseudo-first-order conditions) to give the rate coefficients. For association/dissociation systems such as the title reaction:

$$OH + C_2H_4 \underset{}{\overset{k_1,\ k_{-1}}{\longleftrightarrow}} HOC_2H_4 \qquad \text{(R1, R-1)}$$

analysis is further complicated by the pressure dependence of the rate coefficients. Fundamental problems can arise when the timescales of chemical reaction and energy transfer start to overlap and conventional analysis will not extract reliable rate coefficients. Direct trace fitting using a master equation (ME) for pressure dependent systems overcomes this problem, allows for a global analysis of the experimental data and avoids the need for intermediate processing. The reaction of OH with ethylene, the simplest alkene, is used to test direct trace fitting methodology and to compare the HOC_2H_4 well depth extracted from the kinetic data with values determined by *ab initio* calculations.

Ethylene is an important biogenic emission and inventories suggest that global emissions of ethylene to the atmosphere are dominated by biogenic sources (8-25 Tg), accounting for approximately 75% of the total emissions.[2-3] Anthropogenic sources include industrial emissions (ethylene is extensively used in the manufacture of polymers of wide applicability[4], and also as precursor to many commodity chemicals) and also from combustion sources including transport and biomass burning.[5-6]

When released into the atmosphere, the gas-phase oxidation of ethylene, predominantly initiated by the reaction with hydroxyl radicals, is the major removal process. Ethylene has a relatively short lifetime, τ, with respect to the removal by OH radicals ($\tau \sim 6 - 30$ h) and represents a significant atmospheric OH sink.[7-9] At low temperatures ($T \leq 500$ K) the ethylene + OH reaction proceeds *via* a pressure-dependent OH addition to the π-bond (R1), which is an important reaction in both atmospheric[7, 10] and combustion chemistry.[11,12]

However, at elevated temperatures ($T > 600$ K), the abstraction of a hydrogen atom becomes significant and eventually turns into the major channel of this reaction.[13-14]

$$OH + C_2H_4 \xrightarrow{k_2} C_2H_3 + H_2O \qquad (R2)$$

The abstraction reaction has been studied by Tully[12, 14] who reported Arrhenius parameters of $A_2 = (3.36 \pm 0.64) \times 10^{-11}$ cm^3 molecule^{-1} s^{-1} and an activation energy, E_2, of (24.9 ± 1.2) kJ mol^{-1} from measurements over the temperature range 650 – 901 K.

A further additional process to consider under our experimental conditions is the loss of the HOC_2H_4 adduct. Apart from a small contribution from diffusion out of the observation region (see below), the most likely loss process for the experimental conditions reported below is reaction with oxygen generated from the decomposition of H_2O_2, the OH precursor in our experiments.

$$HOC_2H_4 + O_2 \xrightarrow{k_3} \text{products} \qquad (R3)$$

Reactions R2, R3 and diffusional loss represent the loss processes from the equilibrium system R1, R-1.

The reaction of OH and ethylene has been studied extensively over a wide range of temperatures. Lower temperature data are summarized in the IUPAC evaluation[9] which recommends: $k_1 = 7.8 \times 10^{-12}$ cm^3 molecule^{-1} s^{-1} at 298 K and 1 bar of air and $k_1^{\infty} = 9.0 \times 10^{-12}$ $(T/300)^{-0.85}$ cm^3 molecule^{-1} s^{-1} over the temperature range 100-500 K. As mentioned above, at higher temperatures the abstraction reaction (R2), which has a positive activation energy, starts to become significant, eventually becoming the dominant channel and hence the overall reaction starts to have a positive temperature dependence. The direct laser flash photolysis/ laser induced fluorescence (LFP/LIF) study by Tully is the most relevant to this work.[14] At higher temperatures, measurements have been made *via* less precise methods such as shock tube initiation with end product analysis. The high temperature measurements of Vasu et al.[15], of Westbrook et al.[16] and Srinivasan et al.[11] are broadly consistent with the 650 - 901 K measurements of Tully.[14] The only other direct measurement of k_2 at relevant temperatures by Liu et al.[13] predicts significantly more abstraction than Tully.

Addition and dissociation reactions, such as (R1) are an important class of reactions where the observed rate coefficient is pressure dependent. The OH + ethylene reaction proceeds via a chemically activated intermediate HOC_2H_4*.

$$OH + C_2H_4 \xrightarrow{k_{1a}} HOC_2H_4^* \qquad \text{(R1a)}$$

The collisional stabilization of the HOC_2H_4* adduct competes with the unimolecular decomposition of the HOC_2H_4* adduct (R-1a). The competition between the excited adduct stabilization (dependent on bath gas concentration) and decomposition leads to the observed pressure dependence of the rate coefficients for the formation (k_1) and decomposition (k_{-1}) of the adduct, complicating the extraction of thermodynamic and kinetic parameters. The pressure dependence of such reactions is best modelled by a master equation. Solution of the ME yields, among other things, the chemically significant eigenvalues (CSE) from which, under certain conditions, rate coefficients can be derived and compared with experiment.

However, direct comparison between experimental and modelled quantities is often complicated by several issues, with the effect that the concentrations of reagents may be determined by more than the target reaction and an extension of the ME model is required to account for additional processes. These processes might include diffusion from the observation region and adsorption of reactants and products onto reactor walls. For the present system, the

flash photolysis study of reaction (R1), there is an additional complication; OH will react with ethylene, but also with the OH precursor (e.g. H_2O_2).

$$H_2O_2 + hv \rightarrow 2OH \quad \text{(R4)}$$

$$OH + H_2O_2 \xrightarrow{k_5} H_2O + HO_2 \quad \text{(R5)}$$

As the precursor concentration is usually kept constant and is in excess compared to the radical concentration, diffusion (which can be approximated to a first order process) and reaction with the precursor can be combined in a single first order process with rate coefficient, k_{loss}. Under conditions where only the forward reaction is relevant, the rate of decay of OH with excess C_2H_4 is given by:

$$-\frac{d[OH]}{dt} = k_1[OH][C_2H_4] + k_{loss}[OH] = k_{obs}[OH] \quad \text{(E1)}$$

Solution of this differential equation gives:

$$[OH]_t = [OH]_0 e^{-k_{obs}t} \quad \text{(E2)}$$

where the observed rate coefficient, k_{obs}, for the OH decay is given by:

$$k_{obs} = k_1[C_2H_4] + k_{loss} \quad \text{(E3)}$$

In the conventional approach, a plot of k_{obs} *vs* $[C_2H_4]$ at a constant precursor concentration and a particular temperature and pressure, gives the target rate coefficient, k_1, which can then be compared with the ME prediction for those conditions of temperature and pressure. The general approach to such fitting is shown schematically in Figure 1.[17]

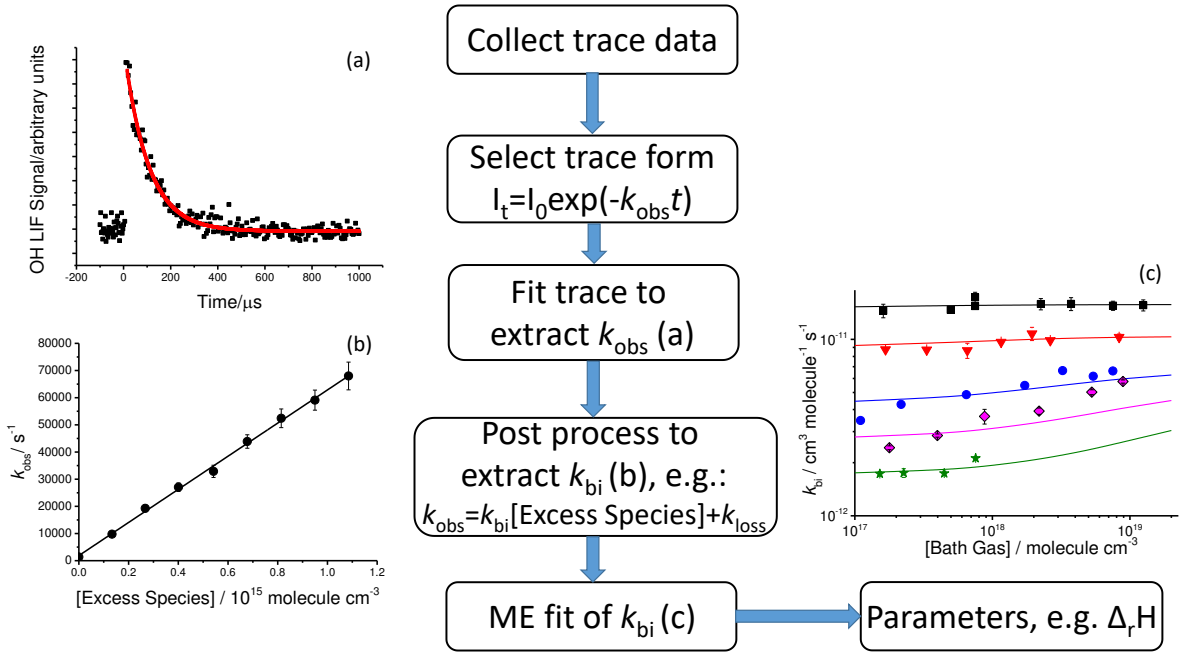

Figure 1. Fitting workflow conventionally used to extract parameters from experimental traces.[17]

The workflow begins by collecting trace data, which are then fitted, by some third-party tool, to an assumed functional form such as (E2). This form is often rationalized on the basis of the system and experience, as is done above, and it is usually a sum of exponentials the parameters of which can be equated with some assumed phenomenological model. The product of the fitting process is usually an estimate of the rate coefficients of the phenomenological model which will be functions of the conditions (pressure and temperature) at which the individual traces were obtained (panel (a) in Figure 1). These rate coefficients often have to be further processed to account for experimental artefacts (diffusional loss, reaction with precursor), as discussed above (panel (b)). These final rate coefficient values are then used in a ME fit where the experimental rate coefficients are compared to rate coefficients obtained from the CSE analysis (panel (c)) and kinetic parameters, such as barrier heights or collision parameters, are determined by a non-linear least squares method of some description.

Under most conditions the CSEs are well separated from those controlling energy transfer (internal energy relaxation eigenvalues, IERE). However, it is possible, particularly at high temperature, that the eigenvalue sets can merge. Under these conditions the temporal profile of the reaction species will not be solely determined by the reaction rate coefficients and simple analytical functions (e.g. exponential or biexponential decays of reagent) are no longer applicable. Thus, if such decays are fit to an analytical function derived from the expected chemical reactions, then significant errors can occur. An important feature of the ME is that its solution yields a detailed description of the time evolution of the system in terms of energy grain populations, which in turn can be integrated to give the detailed time evolution of species concentrations – in effect theoretical decay traces. These traces contain contributions from all eigenvalues, and so, if there is eigenvalue overlap, such theoretical traces will properly include this contribution. These traces can therefore be compared with the experimental data directly and used in a global fitting exercise based on the ME which will automatically account for merged eigenvalue sets and from which the chemical parameters can be extracted.

As well as being of practical interest in its own right, the structural and chemical simplicity of ethylene makes the study of the OH-ethylene reaction a benchmark for testing and validating analytical methods and theoretical calculations[18-20]. In this paper, as well as reporting new experimental data recorded over a wide range of temperature (563 – 723 K) and pressure (58 – 250 Torr N_2) where equilibration between k_1 and k_{-1} can be observed, we test the direct, global fitting of trace data. We have extended the ME programme MESMER[21] to account for the additional chemistry of (R2), (R3) and (R5), and have directly, globally, fitted the experimental trace data to determine $\Delta_r H$ for the formation of the HOC_2H_4 adduct which is

compared with high level *ab initio* calculations. This data analysis method represents a significant step forward in the ability to analyse relatively complex kinetic problems and allows not only the determination of thermochemical and kinetic parameters, but also a mechanistic evaluation of the system.

Methodology

Experimental Study

Experiments were carried out using a multiport, low pressure, slow flow reaction cell, where the OH was generated from 248 nm excimer (LPX200) laser flash photolysis of hydrogen peroxide (R4). The OH radicals were monitored *in situ* by on-resonance laser induced fluorescence, excited by a dye laser (Continuum Precision Scan II YAG pumping a Sirah dye laser at 532 nm with frequency doubling of the ~616 nm output) tuned to the strongest transitions close to 308 nm with the fluorescence collected by a photomultiplier tube mounted perpendicular to the photolysis and probe laser beams. The OH time traces were obtained by scanning in time the dye laser probe pulse with respect to the excimer laser, where typically 200 time points were collected, where each time point was the average from 3 – 12 samples. Further details on the system can be found in previous publications.[22-24]

Ethylene (Air Products, technical grade), the OH precursor (H_2O_2, 50% (w/w) Sigma Aldrich) and the carrier gas (N_2, BOC oxygen free) were flowed into the reaction cell using calibrated mass flow controllers. Typical experimental pressures ranged from 50 to 250 Torr of N_2. The hydrogen peroxide was delivered to the reaction cell using a pressure regulated glass bubbler that is located before a mass flow controller. All the H_2O_2 is lost inside the metal mass flow controller until the flow is ≥ 0.5 L/min; typically the flow was close to 1 L/min. The initial OH concentration was estimated to be ~ 1×10^{12} molecule cm^{-3}. This is estimated from the [H_2O_2] (~ 10^{14} molecule cm^{-3}), which is assigned from the OH removal in the absence of C_2H_4, the measured excimer energy (~50 mJ cm^{-2} $pulse^{-1}$) and the known H_2O_2 cross-section at 248 nm.[25]

In this work, experiments were conducted at sufficiently high temperatures ($T \geq 560$ K) such that the equilibrium between OH/ethylene and the HOC_2H_4 adduct was established. Previous studies show that the thermochemistry of the reaction is significantly sensitive to such measurements.[1, 26]

Ab Initio Calculations

Molecular structures and properties of the relevant species were computed with the M06-2X density functional theory method and the aug-cc-pVTZ version of Dunning's correlation consistent basis sets. Redundant internal coordinates were optimized using the Berny algorithm with the aid of the Gaussian 09 D.01 computational suite. Force-constant matrices, rotational constants, harmonic vibrational frequencies and zero-point energies required for ME calculations were all calculated with the M06-2X/aug-cc-pVTZ methodology. High performance coupled cluster calculations with single, double and triple excitations, the triples described perburbatively (CCSD(T)), were undertaken for a more accurate estimate of the single point energies of the M06-2X/aug-cc-pVTZ stationary points. The single point energies were extrapolated to the complete basis set limit (CBS) using the aug-cc-pV*X*Z basis sets (*X*=2,3,4) and a mixed Gaussian/exponential extrapolation scheme as proposed by Peterson et al.[27] The enthalpy of formation of the adduct, $\Delta_R H_{0K}(C_2H_4\text{-}OH)$, was calculated with this methodology and its value of 111.4 kJ mol^{-1} will be used for a comparison against the experimental determination providing validation of the relative accuracy of the novel analytical method and the *ab initio* calculation.

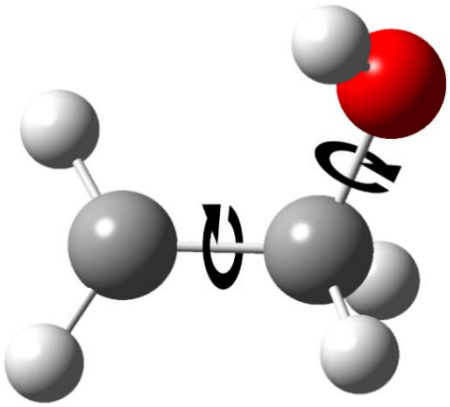

Figure 2. Internal rotations described with the hindered rotor approach for the C_2H_4-OH adduct

As detailed in previous work on the isoprene + OH reaction[28], the hindered rotor approximation was implemented here for the description of two internal rotations of the C_2H_4-OH adduct, related to small harmonic vibrational frequencies (< 350 cm^{-1}). Figure 2 shows the rotations described with the hindered rotor approach. For rotation around the C-C bond the internal rotor is assigned a periodicity of 2.[29-30] The potential was constructed through a relaxed scan of the dihedral angle respective to the rotation, with steps of 15°. A partial structure

optimization was performed at the end of every step, until a 360° coverage was obtained. Having obtained the force constant matrix and the hindered rotor potentials, MESMER applies the procedure described by Sharma et al.[31] to project out the modes related to the internal rotations.

The Master Equation

Our understanding of the complex temperature and pressure dependence of the rate coefficients of unimolecular systems has advanced considerably in recent decades due to the application of methods based on the master equation. Detailed discussions of the formulation and solution of the ME can be found elsewhere[32] and only a brief description of the key features of the ME that are relevant to the fitting of experiment data are given here. In brief, the state space of a given system can be partitioned into species and within those species a set of grains that span the energy range of significant population. Each grain is typically a bundle of states (determined from the densities of states of the individual species which in turn are obtained from the properties of *ab initio* calculation as described above) that have similar energies and are assumed to have broadly similar properties. The population of each of these grains are collected together to form a vector $\boldsymbol{\rho}$ which describes the state of the system at any given time.

The ME is an equation of motion for $\boldsymbol{\rho}$ and can be written as:

$$\frac{d\boldsymbol{\rho}}{dt} = \boldsymbol{M\rho} \tag{E4}$$

where the matrix $\boldsymbol{M}$, the transition matrix, describes the rate of transition of population from one grain to another either via collisional activation/deactivation processes or reaction processes such as isomerisations or dissociations. There are two main constraints that apply to Eq. (E4); detailed balance must be obeyed and, for conservative, systems the elements of $\boldsymbol{\rho}$ must sum to unity, that is, there must be mass conservation.

The general solution of Eq. (E4) is,

$$\boldsymbol{\rho} = \boldsymbol{U}e^{\boldsymbol{\Lambda t}}\boldsymbol{U^{-1}\rho}_0 \tag{E5}$$

where $\boldsymbol{\rho}_0$is the initial population of the system, $\boldsymbol{\Lambda}$ is a diagonal matrix of the eigenvalues of $\boldsymbol{M}$, and $\boldsymbol{U}$ is a matrix of the associated eigenvectors, that is $\boldsymbol{MU} = \boldsymbol{U\Lambda}$. This solution will be the basis of the extended discussion below, but it is of interest to discuss briefly how this solution has been exploited in other ways. One of the principal objectives of an ME analysis is to extract macroscopic rate coefficients for the reactions that define the system being modelled. The problem was first addressed by Bartis and Widom[33] and subsequently extended by Blitz et al.[17] and Miller and Klippenstein.[34-36] This analysis exploits the properties of the eigenvalue

spectrum of $\boldsymbol{M}$ which is often observed to partition into two parts, a set referred to as the internal energy relaxation eigenvalues (IERE), which, as the name suggests, describes the relaxation of the internal energy of the system, and a second set referred to as the chemically significant eigenvalues (CSE) which describes the evolution of the chemistry in the system. If the division in order of magnitude between these two sets is sufficiently large, which is typically the case at low to moderate temperatures, then a set of phenomenological rate coefficients can be obtained that depend only on the CSEs and their associated eigenvectors.

The workflow (as described in the introduction, Figure 1), or something similar, has been employed by a number of groups including ourselves with mostly satisfactory results.[37-38] However, there are a number of weaknesses in this workflow. The principal weakness is in the selection of the functional form to fit to the traces. This functional form is most often a combination of exponential decay terms that are obtained by considering a hypothesized reaction mechanism. While such forms may be applicable in some circumstances, there is a growing body of evidence[36, 39-40] that this is not always the case. One particular difficulty is where the two sets of IERE and CSE start to merge and there is no clear distinction between energy transfer and reaction events, under these circumstances it becomes difficult to identify rate coefficients. Typically, these two sets merge as the temperature increases, but there is no obvious indicator to identify at what point this happens other than by examining the eigenvalues. In some cases, merging occurs because species in the system have reached equilibrium[36], in other cases there is intrinsic multi-exponential decay.[39] A further difficulty, which became apparent in the H + SO_2[17] study and in the work of Klippenstein and Miller[40] is the notion of 'well skipping', where energy wells that are not directly connected at the macroscopic level, when examined using a ME, are found to have finite rate coefficients for exchange between each other. In addition to this, fitting traces individually introduces the possible problem that there will be some over fitting of the results and may not, depending on how it is done, enforce detailed balance constraints. From a more practical point of view the manipulation of data through several computational tools may also introduce further error into the analysis.

A lot of these difficulties can be mitigated by employing Eq. (E5) directly, that is to say rather than extracting rate coefficients and fitting these to a ME model, use the ME model to produce a decay trace and compare this with experiment directly. To be clear, this approach does not solve the problem of whether a given reaction mechanism is correct, this still needs to be determined, but it will address issues to do with merging eigenvalue sets as all eigenvalues appear in Eq. (E5).

Experimental Results

Figure 3 shows examples of experimental OH traces over a range of temperatures and ethylene concentrations. At the lowest temperature (563 K), the OH decay to the baseline is almost exponential, however, as the temperature increases and the ethylene concentration changes, varying degrees of OH recycling can be observed. The fits to the data are explained in Section 4.2.

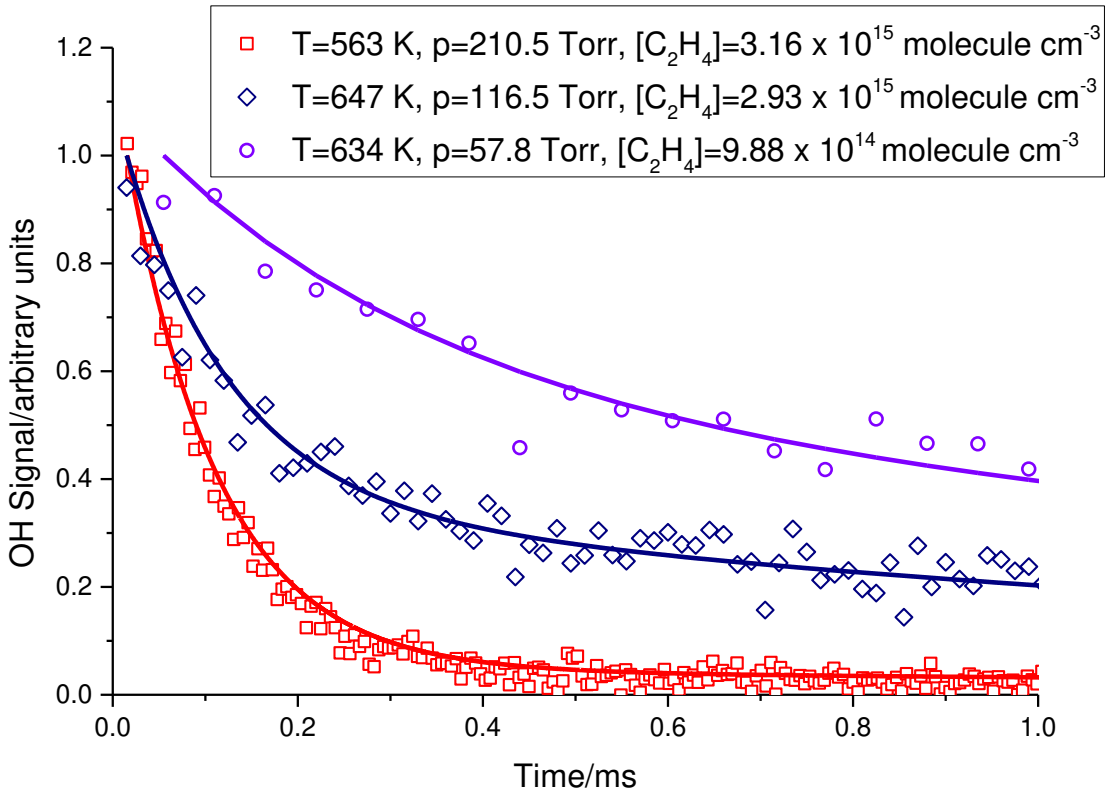

Figure 3. Examples of experimental traces under significantly different conditions. The solid lines are the global ME fits as described below. During the fitting process the amplitude of the calculated trace is altered as described by Eq. (E11). In the plot, the amplitude of each experimental and calculated trace pair has been adjusted by the same, arbitrary factor, one for each pair, to allow them to be displayed together but this has no effect on the temporal behaviour.

Table 1 lists the experimental conditions for which OH traces were recorded; for each temperature and pressure, a range of $[C_2H_4]$ was used. In addition, the laser photolysis fluence was changed to test for secondary chemistry, but there was no significant variation in the

parameters returned, with individual trace analysis, with laser power. A total of 96 traces have been recorded and were used in the ME analysis presented below.

In addition to reaction with ethylene, OH can be lost from the system by diffusion out of the observation region and reaction with the OH precursor, H_2O_2. OH traces for each temperature and pressure were recorded in the absence of ethylene, the resulting profiles were fitted with an exponential decay (i.e. first or pseudo-first-order loss) and the resulting values for k_{loss} are recorded in Table 1.

Table 1. List of experimental conditions

T / K	p / Torr	Number of Traces	$[C_2H_4]$ / 1×10^{15} molecule cm^{-3}	k_{loss} / s^{-1} [a]
563	116	8	1.1 – 8.9	107
563	210	8	1.1 – 8.2	244
580	58	8	1.1 – 8.5	122
610	106	12	0.9 – 7.3	96
614	219	9	1.0 – 6.8	143
634	58	8	1.0 – 7.8	171
647	116	7	1.0 – 7.8	83
672	58	8	0.9 – 7.0	185
676	250	6	2.9 – 8.0	107
694	119	8	0.9 – 7.2	88
696	58	8	0.9 – 6.9	286
723	114	6	2.5 – 6.6	80

a k_{loss} determined from one or two experiments at each condition. Typical error was ± 10%.

Data Analysis

Weighting of data for Master Equation Analysis

Before the details of the fitting of the present data are discussed, some preliminary remarks about the statistics for this fit are appropriate. A typical fitting exercise involves the specification of a model with a set of unknown parameters which are to be determined by

comparison with experimental data. The method that is frequently used in this context is that of least squares, which is described in detail in a number of texts. At the heart of the least squares method is the fitness function χ^2 which is usually written as,

$$\chi^2 = \sum_{i=1}^{N} \left(\frac{y_i - y(t_i; \boldsymbol{\alpha})}{\sigma_i} \right)^2 \tag{E6}$$

where y_i are the dependent experimental values obtained at (time) t_i, $\boldsymbol{\alpha}$ is the set of model parameters associated with the model $y(t; \boldsymbol{\alpha})$ and σ_i are the errors associated with each model point. This expression is typically optimized (minimized) with respect to $\boldsymbol{\alpha}$. The comparison of multiple traces, that is a collections of time series points, taken at different temperature and pressure conditions, requires a modification of Eq. (E6):

$$\chi^2 = \sum_{i=1}^{N_T} w_i \sum_{j=1}^{M_i} \left(\frac{y_{ij} - y(t_{ij},\, T_i, p_i, x_i; \boldsymbol{\alpha})}{\sigma_{ij}} \right)^2 \tag{E7}$$

In Eq. (E7) the index i is over all N_T traces and the index j is over all M_i points within trace i. The term y_{ij} is the jth point of the ith trace recorded at time t_{ij}, for a temperature T_i and pressure p_i and excess species concentrations x_i. The vector $\boldsymbol{\alpha}$, as above, represents the parameters to be estimated. The σ_{ij} are the errors associated with each point and for the current system their values are problematic. The value of y_{ij} is the number of counts recorded by the photo-multiplier tube, and while this process is most likely a Poisson process[41] its parameters, and hence an estimate of σ_{ij}, are unknown. The absence of σ_{ij} means that an independent assessment of the goodness of fit, by comparison with the χ^2 distribution, is not possible.[42] In such circumstances it is necessary to forego this more rigorous approach and adopt the more pragmatic alternative where we assume that σ_{ij} remains constant in a trace and that the fit is average in the sense that $\chi^2/N_{dof} = 1$, N_{dof} being the number of degrees of freedom, in this case the total number of points less the number of parameters floated (which follows from the mean value of the χ^2 distribution being the N_{dof} (See Ref. 42 for details)). The factor w_i is a weight applied to each trace to account for trace-to-trace fluctuations that occur in any real experiment. Ideally this weight should be based on an independent external assessment, but, again, this information is absent. Instead their values are estimated from the mean square of the residuals, s_i^2, obtained from an initial unweighted fit:

$$s_i^2 = \frac{1}{M_i} \sum_{j=1}^{M_i} \left(y_{ij} - y(t_{ij},\, T_i, p_i, x_i; \boldsymbol{\alpha}) \right)^2 \tag{E8}$$

The s_i are then combined to give a set of weights[43]:

$$w_i = \frac{1/s_i^2}{(1/N_T)\sum_j^{N_T} 1/s_j^2} \tag{E9}$$

where N_T is the number of traces. The effect of this weight is to reduce the contribution from noisy data or data that are significantly different from the rest and so might be considered outlier data.

Global Analysis with MESMER

There are two practical problems in fitting the experimental trace data to those calculated from the ME for the present system: i) the removal of OH from the observation volume by non-reactive means or reaction with the OH precursor must be accounted for and ii) the initial value of the [OH] is unknown.

For the present case, the first of these problems requires only a minor alteration to the ME formulation, the introduction of a loss term, as discussed above. To see how this loss term is applied it is necessary to consider the details ME for the present system, which can be written in block matrix format as:

$$\frac{d}{dt}\begin{pmatrix}\boldsymbol{\rho}_c \\ x_A\end{pmatrix} = \begin{pmatrix}\omega_C(\boldsymbol{P_C} - \boldsymbol{I}) - \boldsymbol{K}_C - k_{3,\infty}[\mathrm{O_2}] & k_{1,\infty}[\mathrm{B}]\boldsymbol{\varphi} \\ \boldsymbol{k}_C & -k_{1,\infty}[\mathrm{B}] - k_{\mathrm{loss}} - k_{2,\infty}[\mathrm{B}]\end{pmatrix}\begin{pmatrix}\boldsymbol{\rho}_c \\ x_A\end{pmatrix} \tag{E10}$$

To simplify the presentation of Eq. (E10) the species in the reactions (R1, R-1) are represented as follows: A is OH, B is C_2H_4 and C is the adduct HOC_2H_4, so for example [B] is the concentration of C_2H_4, which is assumed to be in excess. The structure of Eq. (E10) reflects that of Eq. (E5), it is an equation of motion for the population vector $\begin{pmatrix}\boldsymbol{\rho}_c \\ \boldsymbol{x_A}\end{pmatrix}$ which has two parts, the vector $\boldsymbol{\rho}_c$ that describes the grain population of the adduct HOC_2H_4 and x_A the mole fraction of OH. The transition matrix in Eq. (E10) is that of a bimolecular source[32] and the block matrix structure is as follows: the matrix $\omega_C(\boldsymbol{P_C} - \boldsymbol{I})$ describes the energy transfer process of the adduct HOC_2H_4. The $\boldsymbol{K}_C$ matrix is a diagonal matrix that contains the microcanonical rate coefficients for reaction (R-1) and these are determined using the inverse Laplace transform method.[44] The row vector $\boldsymbol{k}_C$ also contains the microcanonical rate coefficients of the system and ensures mass conservation due to reactions (R1, R-1). The vector $\boldsymbol{\varphi}$ represents the chemical activation source distribution which is determined from detailed balance and the rate coefficient $k_{1,\infty}$ is the high-pressure limit rate coefficient of reaction (R1). The rate coefficients $k_{2,\infty}$ and $k_{3,\infty}$ will be discussed below. The rate coefficient k_{loss} accounts for the loss of OH

from the observation region due to factors other than reaction with C_2H_4 and it is assumed that these processes can be approximated as a first order process. As mentioned above, k_{loss} was measured for each temperature and pressure and was directly input into MESMER.

The other practical problem, the absence of knowledge about the initial concentration of OH, was tackled by the following procedure: the ME can generate traces for species by first summing up the elements of the population vector, as given by Eq. (E10), that correspond to the species of interest, in the present case there is only one element for OH so the calculation is simple, and then repeating this for all the times in the trace. The initial condition used for this model trace is that all the population is in OH, that is $x_A = 1$. Direct comparison of the model trace and the experimental trace yields large residual sums (and s_i^2) which can cause the Levenberg-Marquardt algorithm to erroneously optimise parameters to eliminate the largest differences. Instead, a pre-processing step was first done for each trace, in which the amplitude of the model trace was multiplied by a factor, A_i, that minimized the sum of residuals squared between the model and experimental trace, this factor is,

$$A_i = \frac{\sum_j^{M_i} y_{ij} y(t_{ij},\, T_i, p_i, x_i; \boldsymbol{\alpha})}{\sum_j^{M_i} y^2(t_{ij},\, T_i, p_i, x_i; \boldsymbol{\alpha})} \tag{E11}$$

It is important to emphasize that this factor only affects the amplitude of the model trace and leaves its temporal dependence unaffected. This factor was calculated and applied from each trace and residuals obtained after the factor had been applied where then accumulated as part of the overall χ^2 as given by Eq. (E7). At this point a cycle of the Levenberg-Marquardt algorithm was executed to update the parameters $\boldsymbol{\alpha}$. The process was then cycled until convergence was reached for the parameters $\boldsymbol{\alpha}$. This revised fitting sequence is shown in Figure 4. A plot of the data from the final fit showing the experimental and fitted traces is shown in Figure 3.

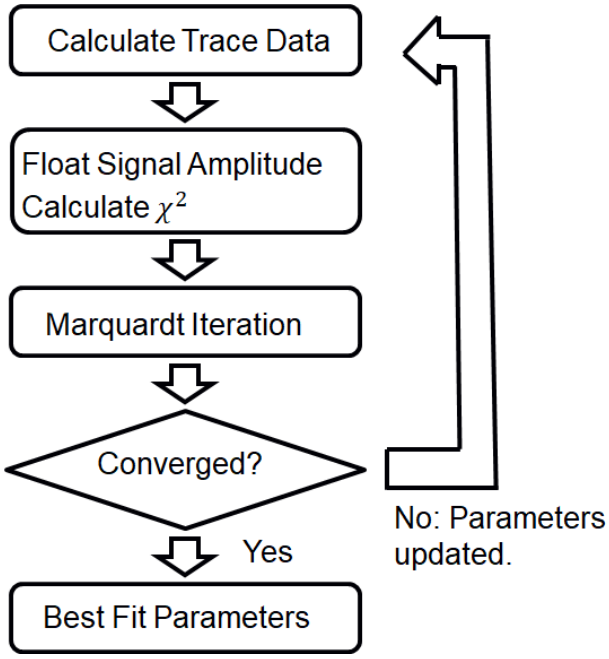

Figure 4. The revised fitting sequence based on the direct comparison of traces.

This fitting sequence was implemented within MESMER and applied to the title reaction. Initially, the data were fit assuming that only the reaction (R1, R-1) occurred in the system and the parameters chosen to be adjusted were: the heat of reaction (R1, R-1) $\Delta_R H_0^0$; the inverse Laplace transform parameters for association reaction (R1), $A_1$and n_1 of the assumed modified Arrhenius functional form $A_1(T/298.0)^{n_1}$ (activation energy being set to zero); and the energy transfer parameters of the adduct, $\langle\Delta E\rangle_{d,298.0}$ and n, the assumed temperature dependent form being $\langle\Delta E\rangle_{d,298.0}(T/298.0)^n$. In all calculations an exponential down model was used to describe energy transfer and a collision frequency based on the Neufeld integral.[45] The details of the parameter set can be found in the MESMER input file which is included in the SI.

The fitting procedure consisted of the following sequence: an initial unweighted fit, that is the w_i were all set to unity, was performed with the object of obtaining a set of s_i^2 to be used to define w_i. Then the data were re-fit with the w_i in place. Finally, the procedure outlined above, of assuming an averagely good fit, was applied in order to adjust the errors obtained from the Levenberg-Marquardt covariance matrix.

The values obtained for this fit are shown in the second column of Table 2 (Model 1). As can be seen the value of $\Delta_R H_0^0$ is significantly greater than the value from our *ab initio* calculation and this difference cannot be rationalized by an overlap in the errors. In addition,

the parameters for energy transfer, in particular the negative index n, are inconsistent with the general observation that $\langle \Delta E \rangle_d$ should increase with temperature.[30, 46]

As discussed in the Introduction there is another possible reaction channel, the direct abstraction of an H-atom by OH (R2). This channel was incorporated into Model 2 by the addition of a loss term for the OH species, indicated in Eq. (E10) by the rate coefficient $k_{2,\infty}$. This rate coefficient was assumed to have a simple Arrhenius like temperature dependence with pre-exponential factor A_2 and activation energy E_2. Both these parameters were floated, along with the original set of parameters (giving a total of 7 parameters) in a second fit, the results of which are also shown in Table 2 (Model 2).

Recorded in Table 2 are the values of χ^2 as reported by MESMER (that is prior to the error factor being determined) and as can be seen there is a significant decrease in the value of χ^2 by a factor of almost two, following incorporation of the abstraction channel, suggesting that Model 2 is a better representation of the data. Also, there is a significant increase in the value of $\Delta_R H_0^0$, it now being much closer to the *ab initio* value. Perhaps more importantly, the energy transfer parameters now appear to be more consistent in sign and value with what has been observed elsewhere.[46] The values of the parameters A_2 ((2.450 ± 0.084) × 10^{-11} cm^3 $molecule^{-1}$ s^{-1}) and E_2 ((22.67 ± 0.24) kJ mol^{-1}) should be compared with those obtained by Tully[14] (A_2 = (3.36 ± 0.64) × 10^{-11} cm^3 $molecule^{-1}$ s^{-1}, E_2 = (24.9 ± 1.2) kJ mol^{-1}). Clearly there is some disagreement regarding A_2 value, but there is better agreement in the value of the activation energy E_2.

Table 2. Parameter values for the three data fits, errors are statistical at the 2σ level.

Parameter	Model 1	Model 2	Model 3
χ^2	0.000339	0.000188	0.000156
$\Delta_R H_0^0$/kJ mol^{-1}	-119.12 ± 0.14	-112.94 ± 0.14	-111.75 ± 0.22
A_1/cm^3 $molecule^{-1}$ s^{-1}	(7.0 ± 4.2) × 10^{-12}	(6.5 ± 2.6) × 10^{-12}	(6.4 ± 2.2) × 10^{-12}
n_1	-0.66 ± 0.96	-0.71 ± 0.58	-0.65 ± 0.48
$\langle \Delta E \rangle_{d,298.0}$/$cm^{-1}$	180 ± 144	213 ± 150	227 ± 160
N	-0.15 ± 0.86	0.33 ± 0.76	0.42 ± 0.76
A_2/ cm^3 $molecule^{-1}$ s^{-1}	N/A	(2.450 ± 0.084)× 10^{-11}	(2.500 ± 0.072) × 10^{-11}
E_2/kJ/mol	N/A	22.67 ± 0.24	23.52 ± 0.24
$k_{3,\infty}$/ cm^3 $molecule^{-1}$ s^{-1}	N/A	N/A	(3.35 ± 0.28) × 10^{-12}

While this modified mechanism greatly improved the agreement in the enthalpy of reaction, one other aspect that was observed experimentally, needs to be considered, that is the presence of a small amount of oxygen from the decomposition of H_2O_2, the OH precursor. This O_2 can react with the nascent adduct (R3), preventing OH regeneration. In order to assess the potential impact of this reaction an additional bimolecular sink term[47] was added to the transition matrix in Eq. (E10), that is $k_{3,\infty}[O_2]$. The exact amount of O_2 produced is unknown, however, studies[48] on the reactions of OH with ethers, where small amounts of O_2 lead to biexponential OH decays, suggest that a value for $[O_2]$ of 1×10^{14} molecule cm^{-3} is typical and the rate coefficient $k_{3,\infty}$was assumed to be temperature independent. A third fit was executed with this additional parameter included. The results of this third fit are reported in Table 2 (Model 3), from which it can be seen there is a further improvement in the value of χ^2 though not as significant as that from fit 1 to fit 2. The value of $\Delta_R H_0^0$ has increased marginally bringing it into better agreement with the *ab initio* value (111.4 kJ mol^{-1}). There is also improved agreement for activation energy E_2 for reaction (R2) when compared to the value of Tully ((24.9 ± 1.2) kJ mol^{-1}).[14] As to the value of $k_{3,\infty}$ it is difficult to draw any conclusions, partly because the concentration of O_2 was assumed and partly because the value is a temperature dependent average.

Discussion

$\Delta_R H_0^0$, HOC2H4

The enthalpy of formation of the HOC_2H_4 adduct determined from direct global fitting (111.75 ± 0.22) kJ mol^{-1}, is in excellent agreement with our theoretically determined value of $\Delta_R H_{0K,HOC2H4}$ of 111.4 kJ mol^{-1}. There have been some previous calculations of this reaction surface, see Table 3. This excellent agreement is accompanied with a relatively small statistical uncertainty associated with the experimental determination and the direct fit. The small uncertainties in the returned parameters are a consequence of carrying out global analysis. However, this does not imply accuracy, which depends on various aspects of the models used in the analysis. As can be seen by the differences between parameters from Models 2 and 3, consideration of minor channels in the chemical model can vary $\Delta_R H_0^0$ by ~ 1 kJ mol^{-1}. The fitting parameters are also sensitive to the methodology used to calculate the density of states and in particular, how low frequency vibrations and hindered rotors are considered. Reactions (R1, R-1) involve a well characterised system and we believe that low frequency vibrations and hindered rotations have correctly been considered. Nevertheless, systematic uncertainties

in our models will introduce a larger error, estimated at ~2 kJ mol^{-1}, than the statistical uncertainty and we therefore report a recommended value for $\Delta_R H_{0K,HOC2H4}$ of (111.8 ± 2.0) kJ mol^{-1}.

Diau et al.[26] report a significantly higher value for $\Delta_R H_{0K,HOC2H4}$ of (124.5 ± 3.3) kJ mol^{-1} from their experimental and fitting study. This higher value originates from the use of a vibration only model, emphasising the importance of accurately treating low frequency vibrations and hindered rotations. A previous *ab initio* calculation on $\Delta_R H_{0K,HOC2H4}$ by Senosiain et al.[19] gives 109.6 kJ mol^{-1}, and a more recent high level calculation by Vereecken (personal communication) gives 113.2 kJ mol^{-1}, see Table 3.

Combining the three recent *ab initio* calculations gives $\Delta_R H_{0K,HOC2H4}$ = 111.4 kJ mol^{-1} and we take the spread of the calculations, ± 2 kJ mol^{-1}, as a good measure of the uncertainty in the calculations. Therefore there appears to be excellent agreement between the values for the experimental $\Delta_R H_{0K,HOC2H4}$ = (111.8 ± 2.0) kJ mol^{-1} and theoretical $\Delta_R H_{0K,HOC2H4}$ = (111.4 ± 2.0) kJ mol^{-1}. This can now be viewed as the new benchmark in comparing experiments and theory.

Table 3. Heat of formation of HOC_2H_4

Study	Method	$\Delta_R H_{0K,HOC2H4}$ / kJ mol^{-1}
This study	Direct trace fitting to experimental, equilibrium data	111.8 ± 2.0
This study	*Ab initio* calculation, CCSD(T) /CBS//M06-2X/aug-cc-pVTZ	111.4
Vereecken (personal communication) 2019	*Ab initio* calculation, CCSD(T) /CBS(DTQ)//M06-2X/aug-cc-pVTZ	113.2
Senosiain et al.[19] 2006	*Ab initio* calculation, CBS-RQCISD(T)	109.6
Cleary et al.[7] 2006	*Ab initio* calculation, DFT-BH&HLYP/6-311 + G(3df,2p)	115.1
Hippler et al.[49] 2000	*Ab initio* calculation, QCISD(T)/6-311 + G(3df,2p)	109.2
Diau et al.[26]	Experiment and fitting.	124.5 ± 3.3 [(a)]

a) The value quoted by Diau et al. at 298 K has been adjusted to 0 K.

The High Pressure Limit for R1: $k_{1a}^{\infty}(T)$

While the focus of this study was on $\Delta_R H_{0K,HOC2H4}$, it is observed from Table 2 that $k_{1a}^{\infty}(T)$ (A_{1a} and n_{1a}) is defined, which is a consequence of the significant ranges over which temperature

and pressure were varied, see Table 1. The IUPAC recommended value for $k_{1a}^{\infty}(T)$ is 9.0×10^{-12} $(T/300)^{-0.85}$, which is within 10% of our value predicted at 298 K, but is 20% too low at 700 K, where our measurements should best pinpoint k_{1a}^{∞}. While our results explain previous experiments down to room temperature, it is interesting to note that the ME using the parameters in Table 2 massively under predicts the measured rate coefficients in cold temperature Laval experiments, T = 69 – 165 K[50-51]; at 69 K the ME underpredicts the rate coefficient by a factor of 8.3. This result cannot be explained by the uncertainties in our parameters. The explanation is almost certainly related to the fact that R1a is controlled by two transition states (TS): the outer TS that dominates at low temperature and the inner TS is a saddle point located along the potential energy surface closer to the products. Greenwald et al.[18] have developed such a two transition-state model for R1a, where over the range 10 – 400 K the reaction was observed to transition from purely outer to the inner TS. Our measurements are taken at temperatures where the reaction is controlled exclusively by the inner TS and therefore will inadequately extrapolate to the temperatures of the Laval experiments. In fact, our 10% disagreement with the literature at 298 K might be a consequence of the outer TS still operating to a smaller extent.

The Abstraction Channel: k_2

As can be seen in Table 2, pure equilibrium is an inadequate description of the trace data. The abstraction reaction R2 is known in the literature, hence it was added to the mechanism when fitting the trace data. The abstraction rate coefficient k_2 (A_2 and E_2) are in good agreement with the study by Tully[14], where R2 is studied over a similar temperature range. An earlier study by Liu et al.[13] assigned k_2 a factor of three higher than the present measurements. These results are most likely a consequence of not wholly identifying k_2 from k_1. In the present analysis, by tethering the analysis directly to a ME, we ensure that the abstraction channel is being properly recognised. Single trace analysis is not as rigorous at imposing the overall mechanism, so it takes more effort in order to correctly identify each contribution of the system. There is also good agreement between the present study and the shock tube study by Vasu et al.[15], which was carried out at much higher temperature. However, this agreement is partly because Vasu et al. extrapolated their data to room temperature using the dataset from Tully.

Conclusions and Future Developments

The primary objectives of this paper are to report experimental measurements of the OH reaction with ethylene and to demonstrate that the ME can be used to directly, globally and reliably fit primary experimental data such as the experimental decay traces shown in Figure 3. To facilitate this analysis, several changes where implemented in the MESMER ME code to account for secondary chemistry, diffusional loss from the observation region and reaction with the photolytic precursor.

There are a number of advantages of this approach, the most fundamental of which is that the ME can deal with data where chemically significant eigenvalues (CSE) and internal energy relaxation eigenvalues (IERE) are not separated. The excellent agreement between the experimentally determined well depth for HOC_2H_4 formation and well-established *ab initio* calculations demonstrates reliable extraction of data by the method. Separate calculations showed that for range of experimental conditions reported in this study, the CSE and IERE are well separated. We will be extending our studies to systems where CSE and IERE overlap in the future.

Burke et al.[52] have previously used primary kinetic data to constrain the optimization of reaction mechanisms in combustion systems. In this approach rate coefficients are generated from, among other methods, a master equation and are then used as input into rate equation integrator to generate the time evolution of the system. The results of this integration are then compared with the target data which includes primary kinetic data such as the evolution of OH radical concentration. In the current approach the time evolution is generated from the master equation itself which avoids the problems associated with the definition of rate coefficients. As such, and to the best of our knowledge, this is the first example of direct, global fitting to primary experimental data with a ME. This one-step approach avoids the need for multi-step analysis (e.g. extracting bimolecular rate coefficients) avoiding potential sources of error (both procedural and from over fitting of a single trace) and is intrinsically global in its approach to fitting providing a more stringent test of any chemical model.

A limitation on the current method, as well as many other previous approaches, is how to weight the data in each trace. Specifically, as discussed in section 4.1 the values of the σ_{ij} are unknown and, therefore, the standard χ^2 goodness of fit test cannot be used as an indicator of the quality of the fit. New methods of data collection and processing should allow us to have a measure of the actual variance in each data point of each curve and therefore this issue should be addressed soon.

Incorporating complex chemistry directly into the ME is non-trivial and we will be presenting extensions of the above method of analysis in the near future where more complex chemistry can be incorporated. This is done by numerically solving coupled differential equations and calling MESMER to explicitly deal with those reactions which are pressure dependent.[53]

Acknowledgments

The authors are grateful to the Brazilian National Council for Scientific and Technological Development (CNPq, grant reference number 206527/2014-4) for support for DJM and to NCAS. The authors thank Dr Chris Morley and Profs. M. J. Pilling and N.J.B. Green for useful discussions.

Supplementary Information

Included in the supplementary information are the MESMER input and output files and plots of all the experimental traces and fits.

References

(1) Seakins, P. W.; Pilling, M. J.; Niiranen, J. T.; Gutman, D.; Krasnoperov, L. N., Kinetics and thermochemistry of R+HBr = RH+Br reactions - determinations of the heat of formation of C_2H_5, i-C_3H_7, sec-C_4H_9, and t-C_4H_9. *J. Phys. Chem.* **1992,** *96*, 9847-9855.
(2) Guenther, A. B.; Jiang, X.; Heald, C. L.; Sakulyanontvittaya, T.; Duhl, T.; Emmons, L. K.; Wang, X., The Model of Emissions of Gases and Aerosols from Nature version 2.1 (MEGAN2.1): an extended and updated framework for modeling biogenic emissions. *Geoscientific Model Development* **2012,** *5*, 1471-1492.
(3) Morgott, D. A., Anthropogenic and biogenic sources of ethylene and the potential for human exposure: A literature review. *Chem. Biol. Interact.* **2015,** *241*, 10-22.
(4) Benham, E.; McDaniel, M., Ethylene Polymers, HDPE. In *Encyclopedia of Polymer Science and Technology*, 4th ed.; John Wiley & Sons, Inc.: 2002.
(5) Gaffney, J. S.; Marley, N. A.; Blake, D. R., Baseline measurements of ethene in 2002: Implications for increased ethanol use and biomass burning on air quality and ecosystems. *Atmos. Environ.* **2012,** *56*, 161-168.
(6) Baker, A. K.; Beyersdorf, A. J.; Doezema, L. A.; Katzenstein, A.; Meinardi, S.; Simpson, I. J.; Blake, D. R.; Rowland, F. S., Measurements of nonmethane hydrocarbons in 28 United States cities. *Atmos. Environ.* **2008,** *42*, 170-182.
(7) Cleary, P. A.; Romero, M. T. B.; Blitz, M. A.; Heard, D. E.; Pilling, M. J.; Seakins, P. W.; Wang, L., Determination of the temperature and pressure dependence of the reaction OH+C_2H_4 from 200-400 K using experimental and master equation analyses. *PCCP* **2006,** *8*, 5633-5642.
(8) Sander, S. P.; Friedl, R. R.; Golden, D. M.; Kurylo, M. J.; Huie, R. E.; Orkin, V. L.; Moortgat, G. K.; Ravishankara, A. R.; Kolb, C. E.; Molina, M. J.; Finlayson-Pitts, B. J. *Chemical kinetics and photochemical data for use in atmospheric studies*; Jet Propulsion Laboratory: Pasadena, 2003.
(9) Atkinson, R.; Baulch, D. L.; Cox, R. A.; Crowley, J. N.; Hampson, R. F.; Hynes, R. G.; Jenkin, M. E.; Rossi, M. J.; Troe, J., Evaluated kinetic and photochemical data for atmospheric chemistry: Volume II - gas phase reactions of organic species. *Atmospheric Chemistry and Physics* **2006,** *6*, 3625-4055.

(10) Lockhart, J. P. A.; Gross, E. C.; Sears, T. J.; Hall, G. E., Kinetic study of the OH plus ethylene reaction using frequency-modulated laser absorption spectroscopy. *Int. J. Chem. Kinet.* **2019,** *51*, 412-421.
(11) Srinivasan, N. K.; Su, M. C.; Michael, J. V., Reflected shock tube studies of high-temperature rate constants for OH+C_2H_2 and OH+C_2H_4. *PCCP* **2007,** *9*, 4155-4163.
(12) Tully, F. P., Laser photolysis laser-induced fluorescence study of the reaction of hydroxyl radical with ethylene. *Chem. Phys. Lett.* **1983,** *96*, 148-153.
(13) Liu, A. D.; Mulac, W. A.; Jonah, C. D., Pulse-radiolysis study of the reaction of OH radicals with C_2H_4 over the temperature-range 343-1173 K. *Int. J. Chem. Kinet.* **1987,** *19*, 25-34.
(14) Tully, F. P., Hydrogen-atom abstraction from alkenes by OH - ethene and 1-butene. *Chem. Phys. Lett.* **1988,** *143*, 510-514.
(15) Vasu, S. S.; Hong, Z. K.; Davidson, D. F.; Hanson, R. K.; Golden, D. M., Shock tube/laser absorption measurements of the reaction rates of oh with ethylene and propene. *J. Phys. Chem. A* **2010,** *114*, 11529-11537.
(16) Westbrook, C. K.; Thornton, M. M.; Pitz, W. J.; Malte, P. C., A kinetic study of ethylene oxidation in a well-stirred reactor. *Symposium (International) on Combustion* **1989,** *22*, 863-871.
(17) Blitz, M. A.; Hughes, K. J.; Pilling, M. J.; Robertson, S. H., Combined experimental and master equation investigation of the multiwell reaction H+SO_2. *J. Phys. Chem. A* **2006,** *110*, 2996-3009.
(18) Greenwald, E. E.; North, S. W.; Georgievskii, Y.; Klippenstein, S. J., A two transition state model for radical-molecule reactions: A case study of the addition of OH to C_2H_4. *J. Phys. Chem. A* **2005,** *109*, 6031-6044.
(19) Senosiain, J. P.; Klippenstein, S. J.; Miller, J. A., Reaction of ethylene with hydroxyl radicals: A theoretical study. *J. Phys. Chem. A* **2006,** *110*, 6960-6970.
(20) Buczek, A.; Kupka, T.; Broda, M. A.; Zyla, A., Predicting the structure and vibrational frequencies of ethylene using harmonic and anharmonic approaches at the Kohn-Sham complete basis set limit. *J. Mol. Model.* **2016,** *22*.
(21) Glowacki, D. R.; Liang, C. H.; Morley, C.; Pilling, M. J.; Robertson, S. H., MESMER: An open-source master equation solver for multi-energy well reactions. *J. Phys. Chem. A* **2012,** *116*, 9545-9560.
(22) McKee, K. W.; Blitz, M. A.; Cleary, P. A.; Glowacki, D. R.; Pilling, M. J.; Seakins, P. W.; Wang, L. M., Experimental and master equation study of the kinetics of OH+C_2H_2: Temperature dependence of the limiting high pressure and pressure dependent rate coefficients. *J. Phys. Chem. A* **2007,** *111*, 4043-4055.
(23) Onel, L.; Blitz, M. A.; Seakins, P. W., A laser flash photolysis, laser induced fluorescence determination of the rate coefficient for the reaction of OH radicals with monoethanol amine (MEA) from 296 - 510 K. *Journal of Physical Chemistry Letters* **2012,** *3*, 853-856.
(24) Baeza-Romero, M. T.; Glowacki, D. R.; Blitz, M. A.; Heard, D. E.; Pilling, M. J.; Rickard, A. R.; Seakins, P. W., A combined experimental and theoretical study of the reaction between methylglyoxal and OH/OD radical: OH regeneration. *PCCP* **2007,** *9*, 4114-4128.
(25) Vaghjiani, G. L.; Ravishankara, A. R., Photodissociation of H_2O_2 and CH_3OOH at 248 nm and 298 K. *J. Chem. Phys.* **1990,** *92*, 996-1003.
(26) Diau, E. W. G.; Lee, Y. P., Detailed rate coefficients and the enthalpy change of the equilibrium reaction OH + C_2H_4 = HOC_2H_4 over the temperature-range 544-673 K. *J. Chem. Phys.* **1992,** *96*, 377-386.
(27) Peterson, K. A.; Woon, D. E.; Dunning, T. H., Benchmark calculations with correlated molecular wave-functions .4. The classical barrier height of the H+H_2 reaction. *J. Chem. Phys.* **1994,** *100*, 7410-7415.
(28) Medeiros, D. J.; Blitz, M. A.; James, L.; Speak, T. H.; Seakins, P. W., Kinetics of the reaction of OH with isoprene over a wide range of temperature and pressure including direct observation of equilibrium with the OH adducts. *J. Phys. Chem. A* **2018,** *122*, 7239-7255.
(29) Hase, W. L.; Schlegel, H. B., Resolution of a paradox concerning the forward and reverse rate constants for C_2H_5 = H+C_2H_4. *J. Phys. Chem.* **1982,** *86*, 3901-3904.
(30) Hanninglee, M. A.; Green, N. J. B.; Pilling, M. J.; Robertson, S. H., Direct observation of equilibration in the system H+C_2H_4 = C_2H_5 - standard enthalpy of formation of the ethyl radical. *J. Phys. Chem.* **1993,** *97*, 860-870.

(31) Sharma, S.; Raman, S.; Green, W. H., Intramolecular Hydrogen Migration in Alkylperoxy and Hydroperoxyalkylperoxy Radicals: Accurate Treatment of Hindered Rotors. *J. Phys. Chem. A* **2010,** *114*, 5689-5701.
(32) Robertson, S. H., Foundations of the Master Equation. *Comprehensive Chemical Kinetics* **2019,** *43*, 291-361.
(33) Bartis, J. T.; Widom, B., Stochastic-models of interconversion of 3 or more chemical species. *J. Chem. Phys.* **1974,** *60*, 3474-3482.
(34) Georgievskii, Y.; Miller, J. A.; Burke, M. P.; Klippenstein, S. J., Reformulation and solution of the master equation for multiple-well chemical reactions. *J. Phys. Chem. A* **2013,** *117*, 12146-12154.
(35) Miller, J. A.; Klippenstein, S. J., From the multiple-well master equation to phenomenological rate coefficients: Reaction on a C_3H_4 potential energy surface. *J. Phys. Chem. A* **2003,** *107*, 2680-2692.
(36) Miller, J. A.; Klippenstein, S. J., Determining phenomenological rate coefficients from a time-dependent, multiple-well master equation: "species reduction" at high temperatures. *PCCP* **2013,** *15*, 4744-4753.
(37) Seakins, P. W.; Robertson, S. H.; Pilling, M. J.; Slagle, I. R.; Gmurczyk, G. W.; Bencsura, A.; Gutman, D.; Tsang, W., Kinetics of the unimolecular decomposition of iso-C_3H_7 - weak collision effects in helium, argon, and nitrogen. *J. Phys. Chem.* **1993,** *97*, 4450-4458.
(38) Hoyermann, K.; Mauss, F.; Olzmann, M.; Welz, O.; Zeuch, T., Exploring the chemical kinetics of partially oxidized intermediates by combining experiments, theory, and kinetic modeling. *PCCP* **2017,** *19*, 18128-18146.
(39) Wang, H. M.; You, X. Q.; Blitz, M. A.; Pilling, M. J.; Robertson, S. H., Obtaining effective rate coefficients to describe the decomposition kinetics of the corannulene oxyradical at high temperatures. *PCCP* **2017,** *19*, 11064-11074.
(40) Miller, J. A.; Klippenstein, S. J., Master equation methods in gas phase chemical kinetics. *J. Phys. Chem. A* **2006,** *110*, 10528-10544.
(41) Lightfoot, P. D.; Pilling, M. J., Temperature and pressure-dependence of the rate-constant for the addition of H to C_2H_4. *J. Phys. Chem.* **1987,** *91*, 3373.
(42) Press, W. H.; Teukolsky, S. A.; Vitterling, W. T.; Flannery, B. P., *Numerical Recipes in C++*. Cambridge University Press: Cambridge, 2002.
(43) Bevington, P. R. S., *Data Reduction and Error Analysis for the Physical Sciences*. McGraw-Hill: New York, 1969.
(44) Davies, J. W.; Green, N. J. B.; Pilling, M. J., The testing of models for unimolecular decomposition via inverse Laplace transformation of experimental recombination rate data. *Chem. Phys. Lett.* **1986,** *126*, 373-379.
(45) Neufeld, P. D.; Aziz, R. A.; Janzen, A. R., Empirical equations to calculate 16 of transport collision integrals-Ω(L,S)' for Lennard-Jones (12-6) potential. *J. Chem. Phys.* **1972,** *57*, 1100-&.
(46) Seakins, P. W.; Robertson, S. H.; Pilling, M. J.; Wardlaw, D. M.; Nesbitt, F. L.; Thorn, R. P.; Payne, W. A.; Stief, L. J., The temperature and isotope dependence of the reaction of methyl radicals and atomic hydrogen. *J. Phys. Chem.* **1997,** *101*, 9974.
(47) Glowacki, D. R.; Lockhart, J.; Blitz, M. A.; Klippenstein, S. J.; Pilling, M. J.; Robertson, S. H.; Seakins, P. W., Interception of excited vibrational quantum states by O_2 in atmospheric association reactions. *Science (Washington, D. C., 1883-)* **2012,** *337*, 1066-1067.
(48) Potter, D. G.; Blitz, M. A.; Seakins, P. W., A generic method for determining R + O_2 rate parameters via OH regeneration. *Chem. Phys. Lett.* **2019,** *730*, 213-219.
(49) Hippler, H.; Viskolcz, B., Addition complex formation vs. direct abstraction in the OH+C_2H_4 reaction. *PCCP* **2000,** *2*, 3591-3596.
(50) Taylor, S. E.; Goddard, A.; Blitz, M. A.; Cleary, P. A.; Heard, D. E., Pulsed Laval nozzle study of the kinetics of OH with unsaturated hydrocarbons at very low temperatures. *PCCP* **2008,** *10*, 422-437.
(51) Vakhtin, A. B.; Murphy, J. E.; Leone, S. R., Low-temperature kinetics of reactions of OH radical with ethene, propene, and 1-butene. *J. Phys. Chem. A* **2003,** *107*, 10055-10062.
(52) Burke, M. P.; Goldsmith, C. F.; Klippenstein, S. J.; Welz, O.; Huang, H. F.; Antonov, I. O.; Savee, J. D.; Osborn, D. L.; Zador, J.; Taatjes, C. A.; Shepsll, L., Multiscale Informatics for Low-Temperature Propane Oxidation: Further Complexities in Studies of Complex Reactions. *J. Phys. Chem. A* **2015,** *119*, 7095-7115.

(53) Medeiros, D. J. New methods for data analysis of complex chemical systems with practical applications for atmospheric studies. University of Leeds, Leeds, 2019.

TOC Graphic

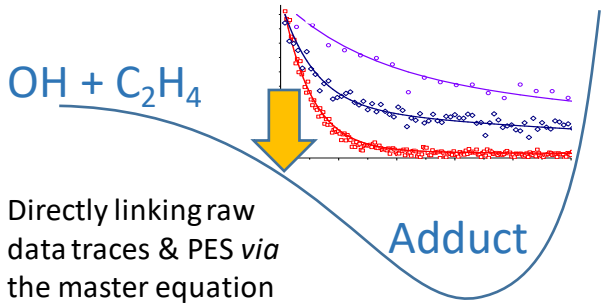

Directly linking raw data traces & PES *via* the master equation